SCARLET · TEV–PEV

Neutrinos, antineutrinos and *inelasticity*

Structure-function model dependence of the inelasticity of TeV–PeV neutrino interactions and of neutrino–antineutrino separation in neutrino telescopes

Rafael C. R. de Lima

with Bruno Duarte da Silva Moreira

UDESC/CCT · Joinville, Brasil

rafael-lima.pages.dev/talks

OUTLINE

Four parts

I IceCube

What the detector measures and how composition enters the analysis

II DIS

Structure functions and the separation of ν and $\bar{\nu}$

III GENIE and SCARLET

Models, implementation and constraints from data

IV Results

Composition shifts, kinematic origin and statistical scale

MAIN QUESTION

Similar means, *different compositions*

How much does the inferred $\nu/\bar{\nu}$ composition change when we change the interaction templates?

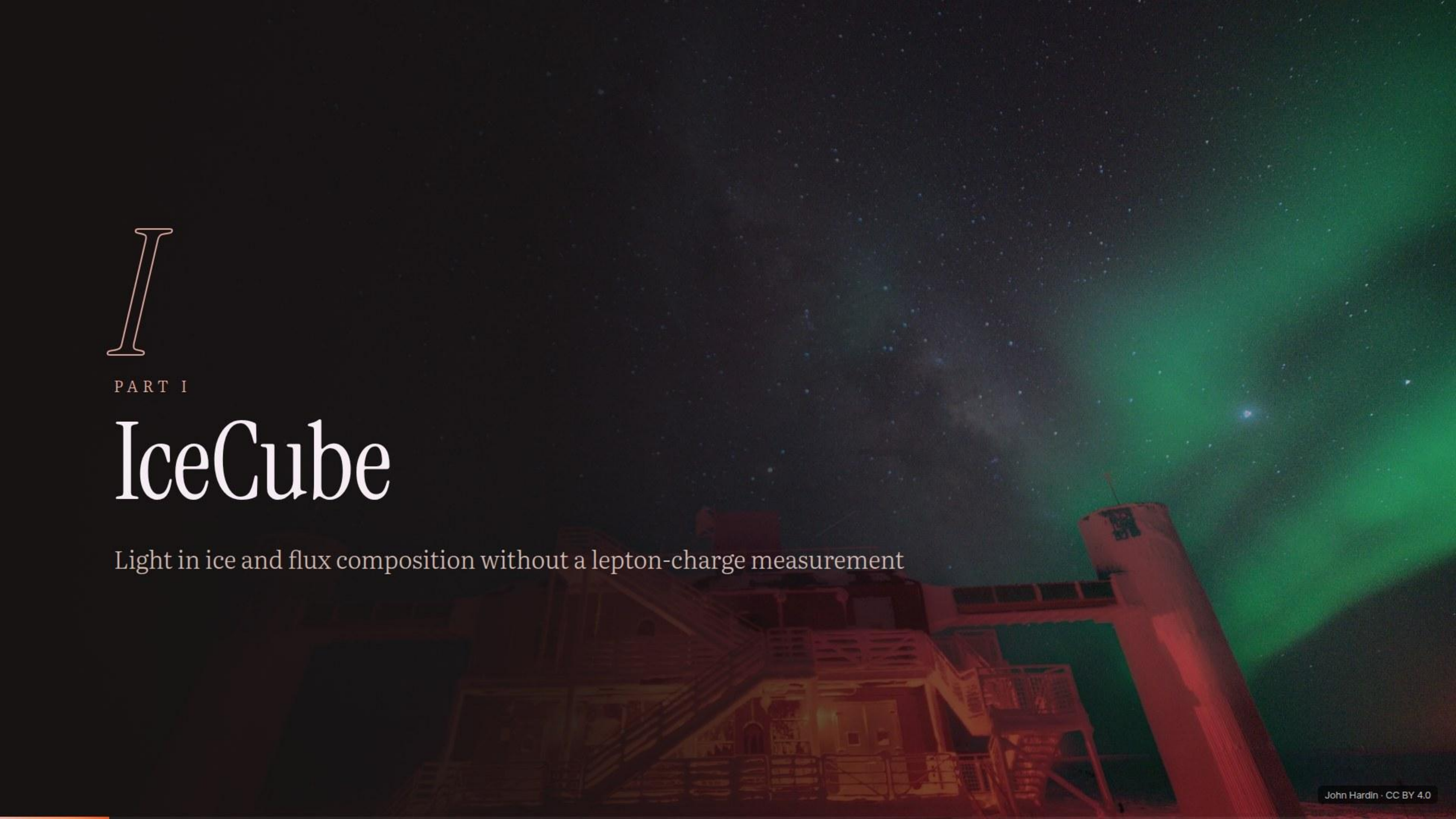
> The shift depends on both the template difference and the remaining separating power.

I

PART I

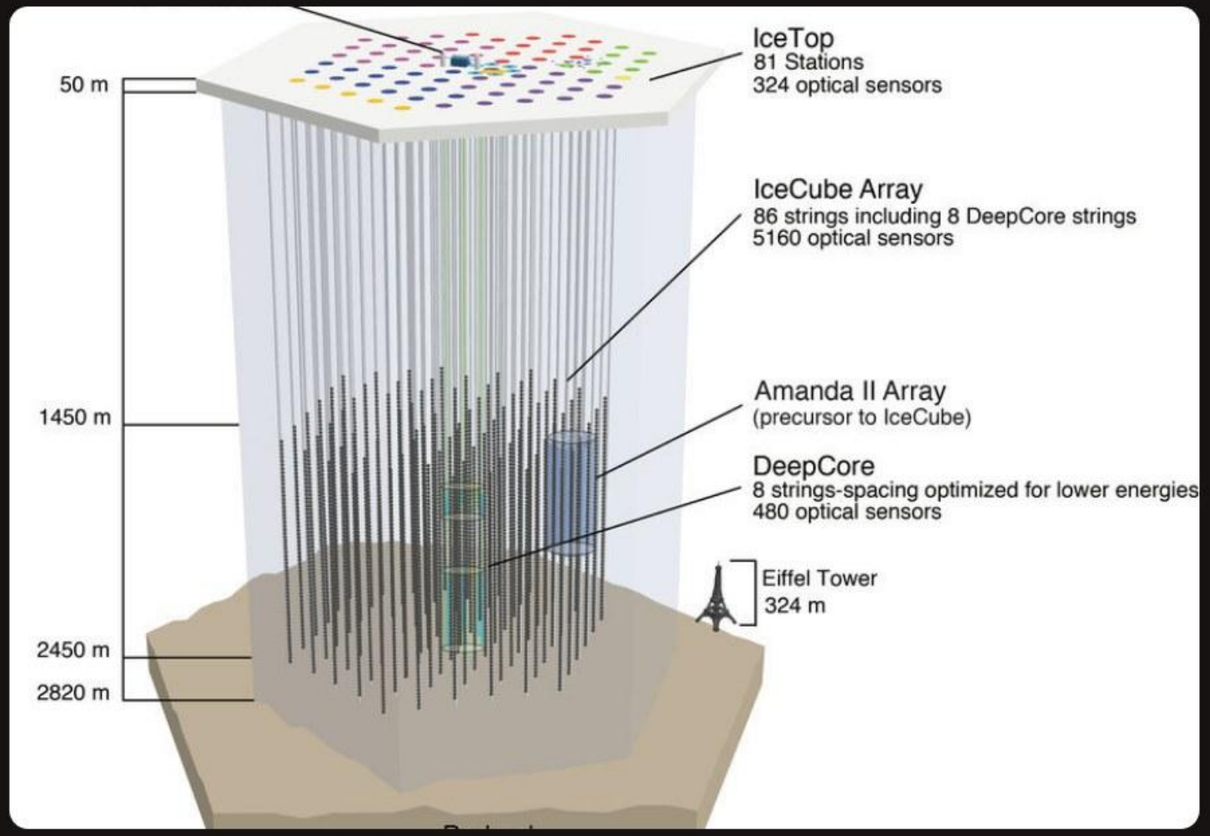
IceCube

Light in ice and flux composition without a lepton-charge measurement



John Hardin · CC BY 4.0

A cubic kilometre of *instrumented ice*



5,160 optical modules on 86 strings.

Sensors at depths of **1,450–2,450 m**.

Charged particles produce Cherenkov light. Signal times and intensities constrain the event geometry and energy.

K. Andeen & M. Plum · IceCube · CC BY 4.0

IceCube · icecube.wisc.edu/science/icecube/

The cascade and muon share *the energy*

$$\nu_\mu + N \rightarrow \mu^- + X \quad \bar{\nu}_\mu + N \rightarrow \mu^+ + X$$

The hadronic cascade receives approximately yE_ν. The muon receives $(1 - y)E_\nu$.

The detector measures light and reconstructs energies. The μ^-/μ^+ charge is unavailable event by event.

IceCube, Phys. Rev. D 99 (2019) 032004 · arXiv:1808.07629

True and *reconstructed* inelasticity

Energy partition · example without smearing



y 0.35 κ 0.90

Example without resolution or containment losses

$$y = E_{had} / E_{\nu}$$

$$y_{vis} = \kappa y / [(1 - y) + \kappa y]$$

Simplified response with full containment

κ represents the cascade response. Migration and selection enter the forward fit.

THE MOTIVATING MEASUREMENT

IceCube already uses *inelasticity*

5

years of contained events

1–100 TeV

approximate inelasticity measurement range

0.77

flux ratio relative to HKKMS, with +0.44/−0.25

> Sensitivity to the atmospheric ratio comes from 770 GeV–21 TeV.

IceCube · arXiv:1808.07629

THREE DISTINCT QUANTITIES

Interaction fraction, event fraction and *flux ratio*

QUANTITY	DEFINITION	INGREDIENTS
f	$\bar{\nu}$ fraction of CC interactions	True distributions at fixed energy
f_{ev}	$\bar{\nu}$ fraction of selected events	Fluxes, cross sections and response
r	Scale on HKKMS $\Phi_{\nu\mu}/\Phi_{\bar{\nu}\mu}$	Joint fit with flux nuisances

> A shift in f does not translate directly into the same shift in r.

II

PART II

DIS

Structure functions determine the distributions that separate ν and $\bar{\nu}$

KINEMATICS

The domain of *Bjorken x and Q^2*

$$Q^2 = 2M\,E_\nu\,xy \qquad W^2 = M^2 + Q^2(1/x - 1)$$

x measures the nucleon momentum fraction sampled by the interaction. Q^2 sets the resolution scale.

$$(M_W^2 / [Q^2 + M_W^2])^2$$

The propagator suppresses Q^2 far above M_w^2

F_2, F_L and xF_3

$$d^2\sigma^{\nu,\bar{\nu}}/dxdy = (G_F^2 ME/\pi)\,(M_W^2/[Q^2+M_W^2])^2$$

$$\times\,[F_2(1-y+y^2/2) - F_L y^2/2 \pm xF_3\, y(1-y/2)]$$

The xF_3 term changes sign between ν and $\bar{\nu}$. Positive F_L suppresses the high-y tail.

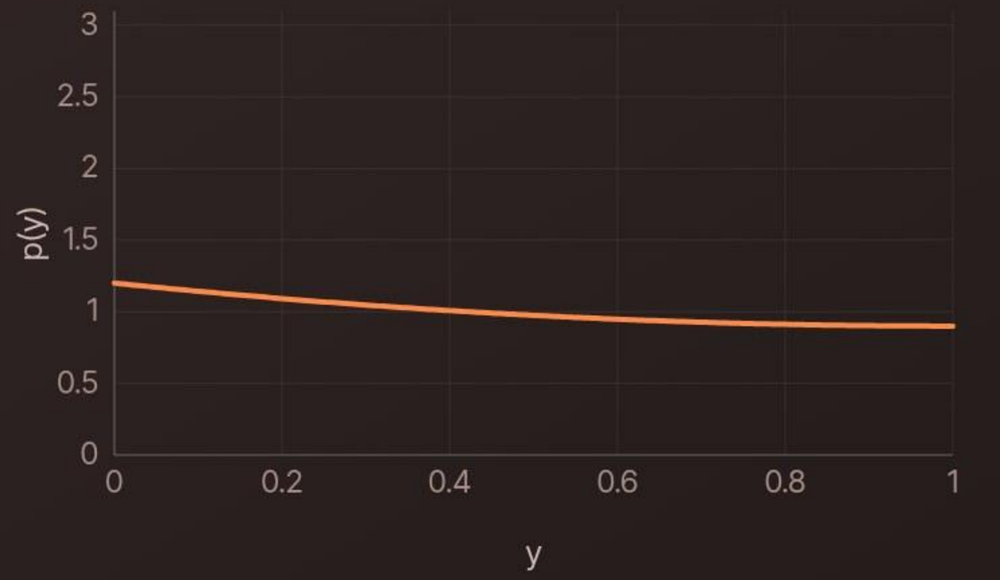
Expression without lepton-mass and target-mass terms. The calculation uses each configuration's prescriptions.

Manuscript · eq. (2.1)

ANALYTIC ILLUSTRATION

Helicity and the *y distribution*

LO · $F_L = 0$ · no scaling violations



$R = \pm xF_3/F_2$ 0.50

⟨y⟩ 0.4750 analytic normalisation

$$d\sigma/dy \propto 1 - y + y^2/2 + R(y - y^2/2)$$

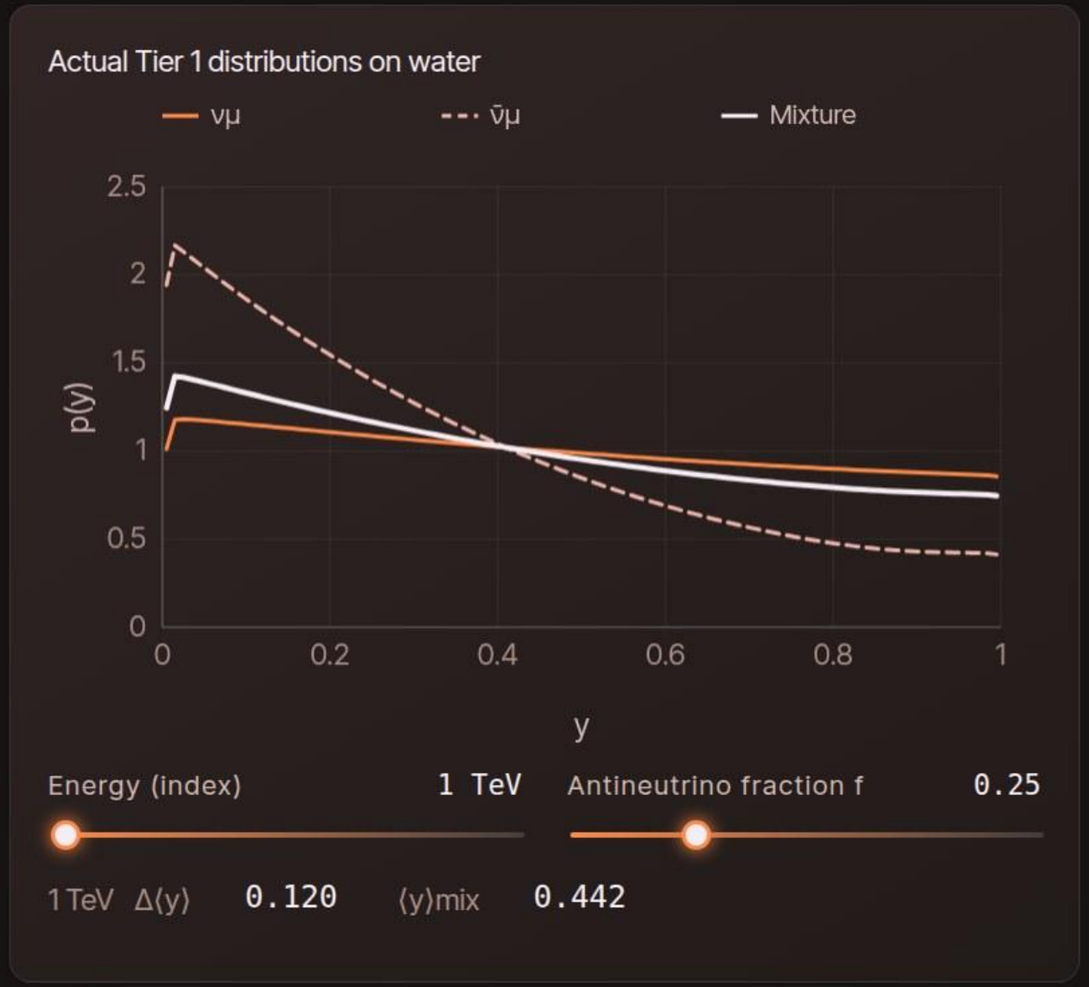
$$\langle y \rangle = (7 + 5R)/(16 + 8R)$$

R = +1: a flat distribution.

R = −1: a distribution proportional to $(1 - y)^2$.

Manuscript · eqs. (2.2)–(2.3)

Composition depends on *the templates*



Paper data · WP-F · 100 bins em y

$$p(y) = (1 - f)p_{\nu}(y) + fp_{\bar{\nu}}(y)$$

The two distributions approach each other as energy increases. The same change in f then produces a smaller shape change.

BIAS MECHANISM

Separation enters *the denominator*

$$\delta f \simeq -\left[(1-f)\delta_{\nu} + f\delta_{\bar{\nu}}\right] / \left[\langle y\rangle_{\nu} - \langle y\rangle_{\bar{\nu}}\right]$$

δ_{ν} and $\delta_{\bar{\nu}}$ are the true mean shifts relative to the template means.

As separation decreases, a small shape mismatch can shift the composition substantially. The full fit uses the entire distribution.

Manuscript · eq. (2.4)

DIPOLE DESCRIPTION

The boson fluctuates into *a quark pair*

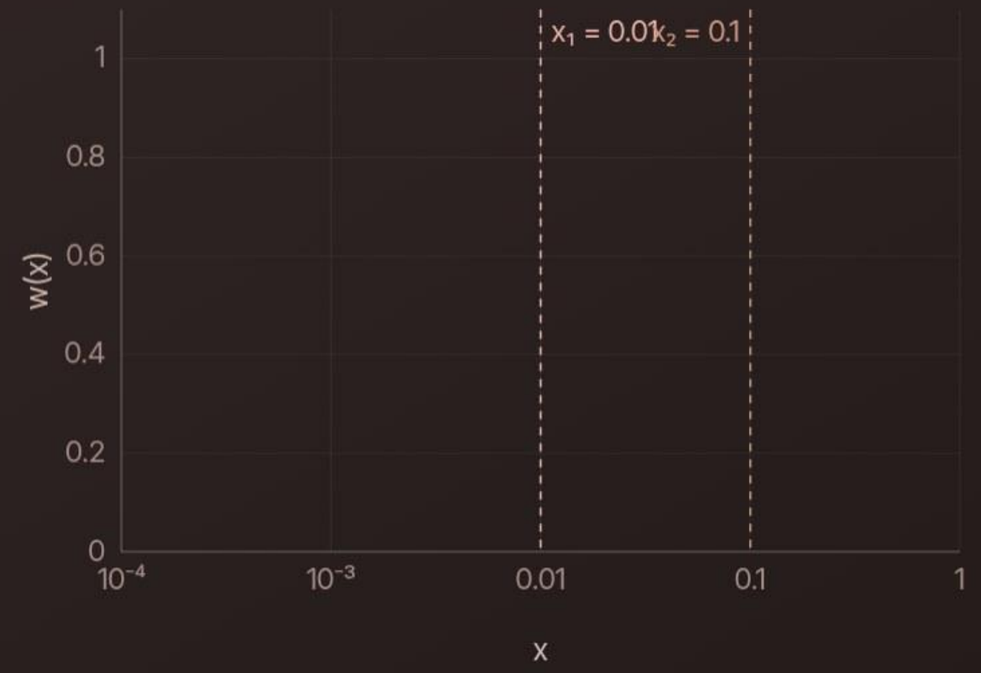
$$F_{T,L} = Q^2/(4\pi^2)\, \Sigma_{q_1 q_2^-} \int d^2r \int dz\, D_{T,L}{}^{V}(z,r)\, \sigma_{qq}(\tilde{x},r)$$

Current wave functions determine the coupling to the pair. The dipole cross section describes its interaction with the target.

BGK includes DGLAP evolution of the gluon. This work uses a HERA fit and three matching prescriptions.

BGK, Phys. Rev. D 66 (2002) 014001 · Manuscript §3

A window between *two descriptions*



Blend weight. Shape variants use edge normalisations.

$$S = wD + (1 - w)C$$
$$w = 1 - t^2(3 - 2t)$$
$$t = \ln(x/0.01)/\ln(10)$$

Below x = 0.01, the dipole part. Above x = 0.1, the conventional description.

Tier 1 preserves the dipole shape inside the window. Tier 2 tests the blend and conventional shape.

Manuscript · eqs. (3.2)–(3.3)

III

PART III

GENIE and SCARLET

A common implementation for structure functions and inference

ARCHITECTURE

The roles of GENIE and *SCARLET*

LAYER	ROLE
GENIE R-3_06_02	Channels, kinematics and event-generation infrastructure
SCARLET · scarlet_physics	Wave functions, dipoles and structure functions
SCARLET · scarlet_genie	Adapters for the GENIE DIS and charm algorithms
SCARLET · analysis	Integration, templates, controls and composition fits

> GENIE remains a dependency. The adapters replace algorithms through configuration.

SCARLET · src/genie_interface · Manuscript §3

One reference and *three dipoles*

MODEL	CONSTRUCTION	STATUS
HEDIS / NLO	HERAPDF1.5 + APFEL	External reference
Tier 1	BGK + valence subtraction + dipole shape	Admitted by the relative criterion
Tier 2	Same BGK, blend and conventional shape	Variations failing the pull condition
Bodek–Yang	GENIE conventional structure functions	Separate comparison

> "Family" includes NLO and the three dipoles. Bodek–Yang is separate.

REACH OF THE DATA

Data constrain *other scales*

DATA SET	x	Q^2 (GEV^2)	ROLE
HERA	≤ 0.01	≤ 650	Dipole fit
NuTeV	0.015, 0.045, 0.08	1–48	Candidate discrimination
TeV–PeV predictions	Multiple regions	~10^2–10^4	Evolution and matching

> The prediction requires extrapolating the fitted inputs. The study quantifies differences between those prescriptions.

Manuscript · §4, Reach of these constraints

Tier 1 passes *by a narrow margin*

NUTEV	χ^2/N ($X \leq 0.1$ / ALL X)	LARGEST PULL
Bodek–Yang	2.18 / 2.29	−5.5σ
Tier 1	1.67 / 1.68	−2.77σ
Tier 1 without 1.032	—	−4.1σ
Tier 1 without radiation	—	−4.3σ

> The criterion was revised with results already known. The factor 1.032 entered with that revision.

Manuscript · Table 1 · Histórico em apêndice / history in appendix

NLO REFERENCE

HEDIS remains *an external reference*

HEDIS VARIANT	NUTEV χ^2/N	CCFR χ^2/N
Nominal	2.54 / 2.87	5.23 / 3.85
× 1.032	2.72 / 3.06	5.23 / 3.85
Iron factor	2.90 / 3.00	2.43 / 2.29
Iron × 1.032	3.09 / 3.20	2.43 / 2.29

> The nuclear factor improves CCFR and worsens NuTeV. Every variant fails the NuTeV criterion.

Manuscript · Table 1

CHARM TREATMENT

An inverted propagator *in G18*

$$G_W^2 \propto (1 + Q^2/M_W^2)^2$$

Form found in AivazisCharmPXSecLO

$$G_W^2 \propto (1 + Q^2/M_W^2)^{-2}$$

Correct propagator dependence

The cross-section effect is ≤ 0.4% up to 1 TeV, but grows when extrapolating G18. HEDIS does not use this model.

The comparisons use charm consistent with each configuration's structure functions.

GENIE issue #558 · Manuscript §3 and appendix C

IV

PART IV

Results

Similar shapes, loss of separation and composition shifts

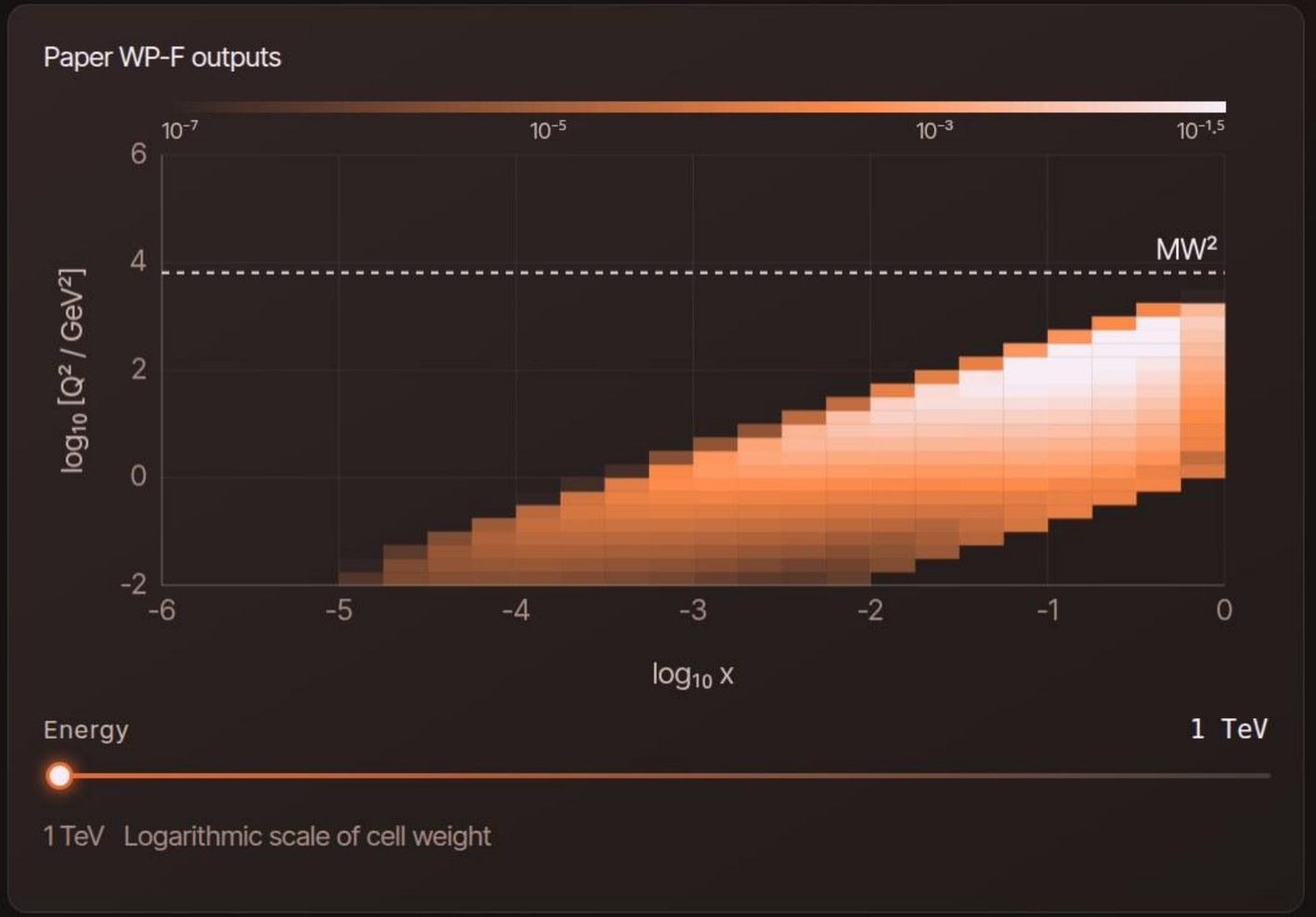
DISTRIBUTION IN X AND Q^2

The kinematic domain changes *with energy*

Tier 1, ν_μ, water. Cross-section fraction per 0.25 × 0.25 decade cell.

x < 0.01: from **3.1%** to **55%** between 1 TeV and 1 PeV.

The occupancy map does not isolate saturation effects.



Paper data · WP-F · Table 2

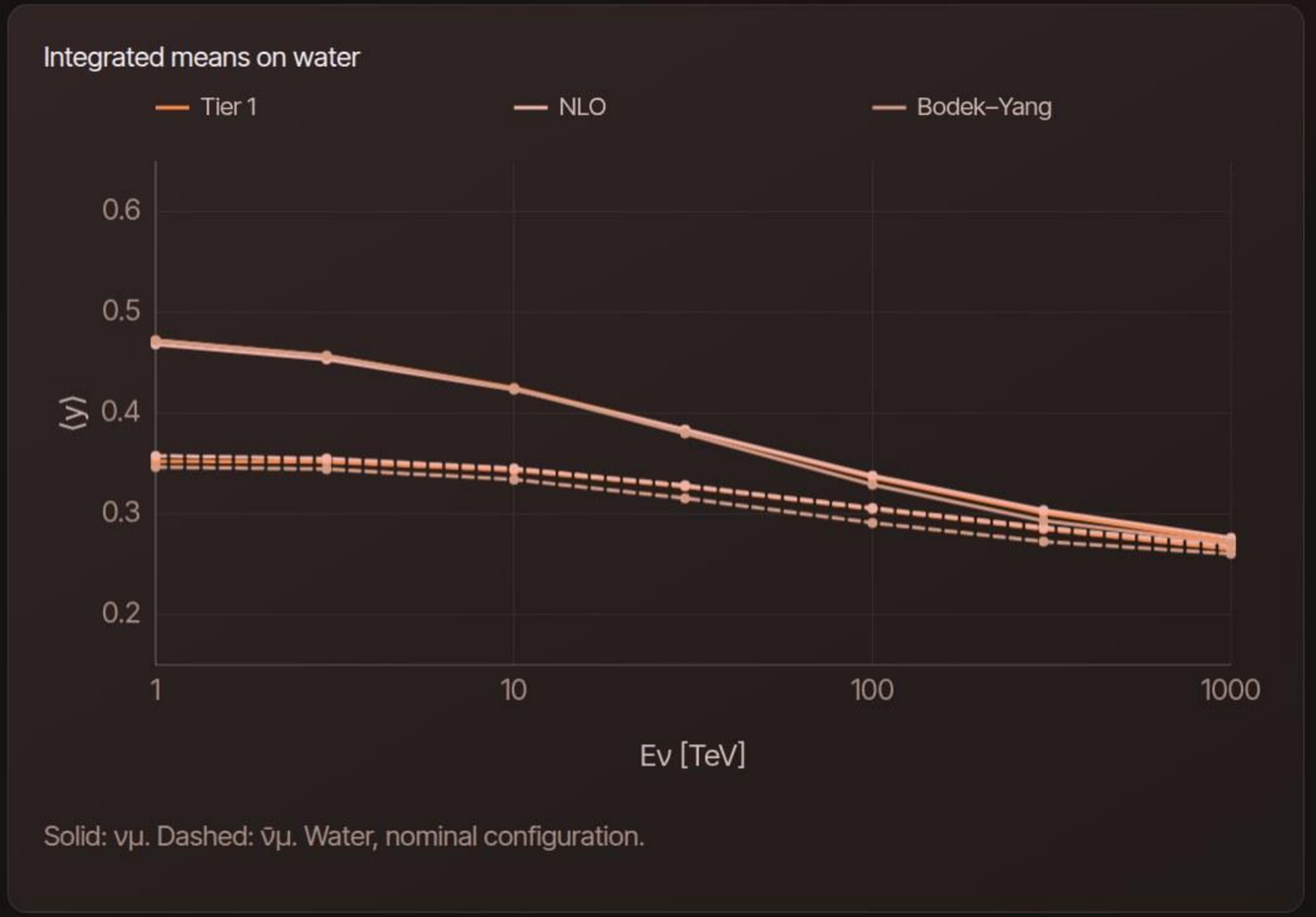
SEPARATING POWER

Δ⟨y⟩ falls from *0.12 to 0.008*

The ν–ν̄ separation decreases far more than the spread of model means.

Within the family, the means differ by at most about **0.005**.

Solid lines: ν.
Dashed lines: ν̄.



Manuscript · Figure 2 · dados WP-F

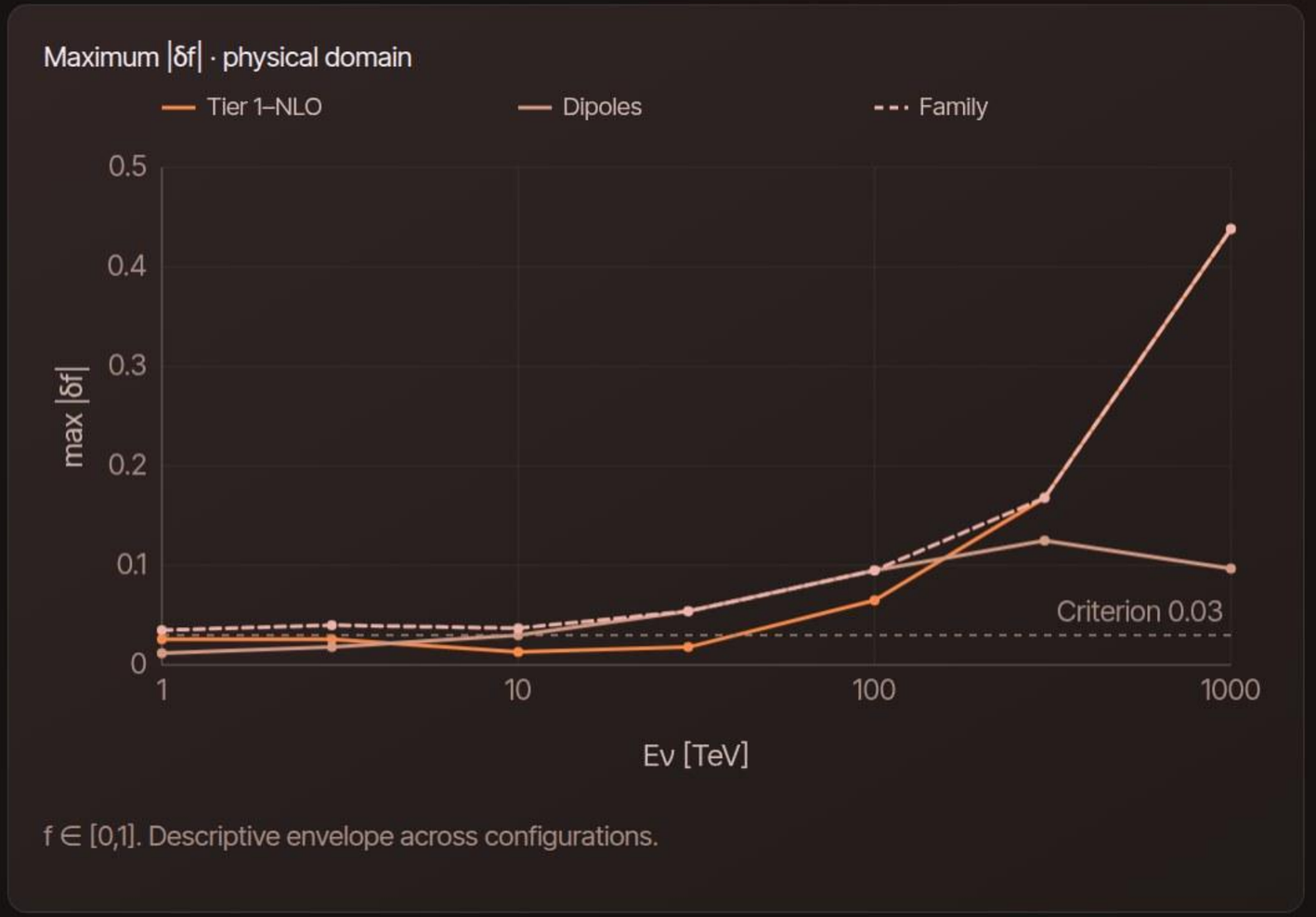
SHAPE FITS

Small differences shift *the fraction*

Templates of A fitted to the expected mixture of B.

Maximum over ordered pairs and f = 0.15–0.50, with 20 bins in y.

The physical fit uses $\mathbf{0 \le f \le 1}$. Large high-energy shifts accompany a loss of information.



f ∈ [0,1]. Descriptive envelope across configurations.

Manuscript · Table 3 · Figure 3

IDENTIFIABILITY

A large bias can occur *without a poor fit*

2.4

$\sigma_f\sqrt{N}$ at 1 TeV

31

$\sigma_f\sqrt{N}$ at 1 PeV

≤ 1.2

deviance for 18 degrees of freedom at exposure N_{bias}

> At the exposure where $|\delta f|$ equals the statistical error, goodness of fit may not reveal the shift.

Manuscript · §5 e Table 3

IMPLEMENTATION CONTROLS

Common *targets and cuts*

E (TeV)	Nominal	Free nucleons	+ W > 2 GeV	+ Q^2 > 1 GeV²
1	0.026	0.021	0.030	0.023
3	0.026	0.019	0.021	0.017
100	0.065	0.049	0.049	0.048
1000	0.438	0.318	0.318	0.317

Maximum $|\delta f|$, Tier 1–NLO. Cuts matter at low energy. Nuclear treatment explains part of the high-energy difference.

Manuscript · Table 4 · physical fits

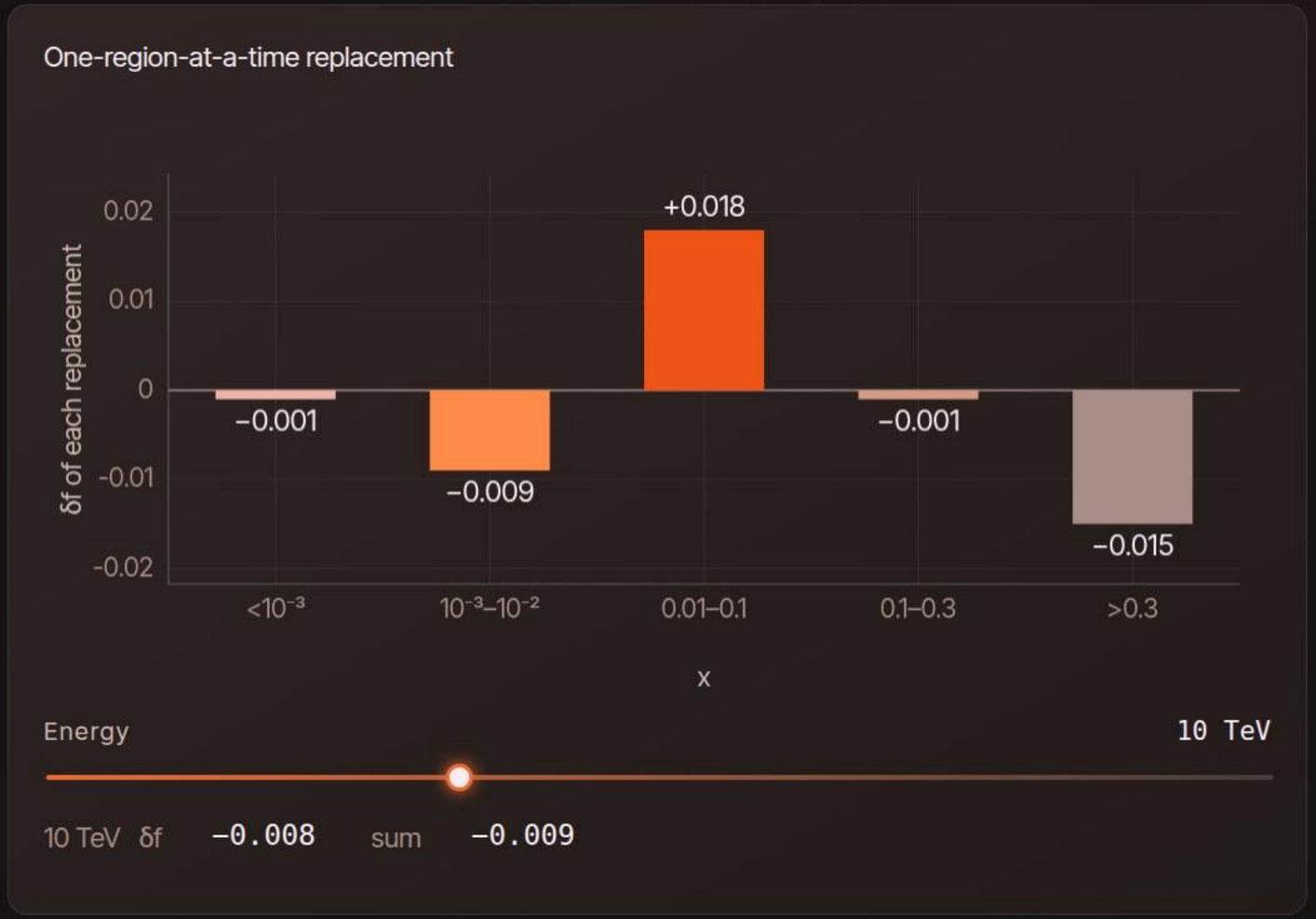
REGIONAL DECOMPOSITION

Contributions in x *can cancel*

Fixed comparison: NLO templates fitted to a Tier 1 mixture with f = 0.25.

Up to 30 TeV: $|\delta f| \leq 0.019$ with cancellations.

Matching dominates at 100 TeV. x < 0.01 dominates from 300 TeV.



Manuscript · Table 5 · controlled replacement

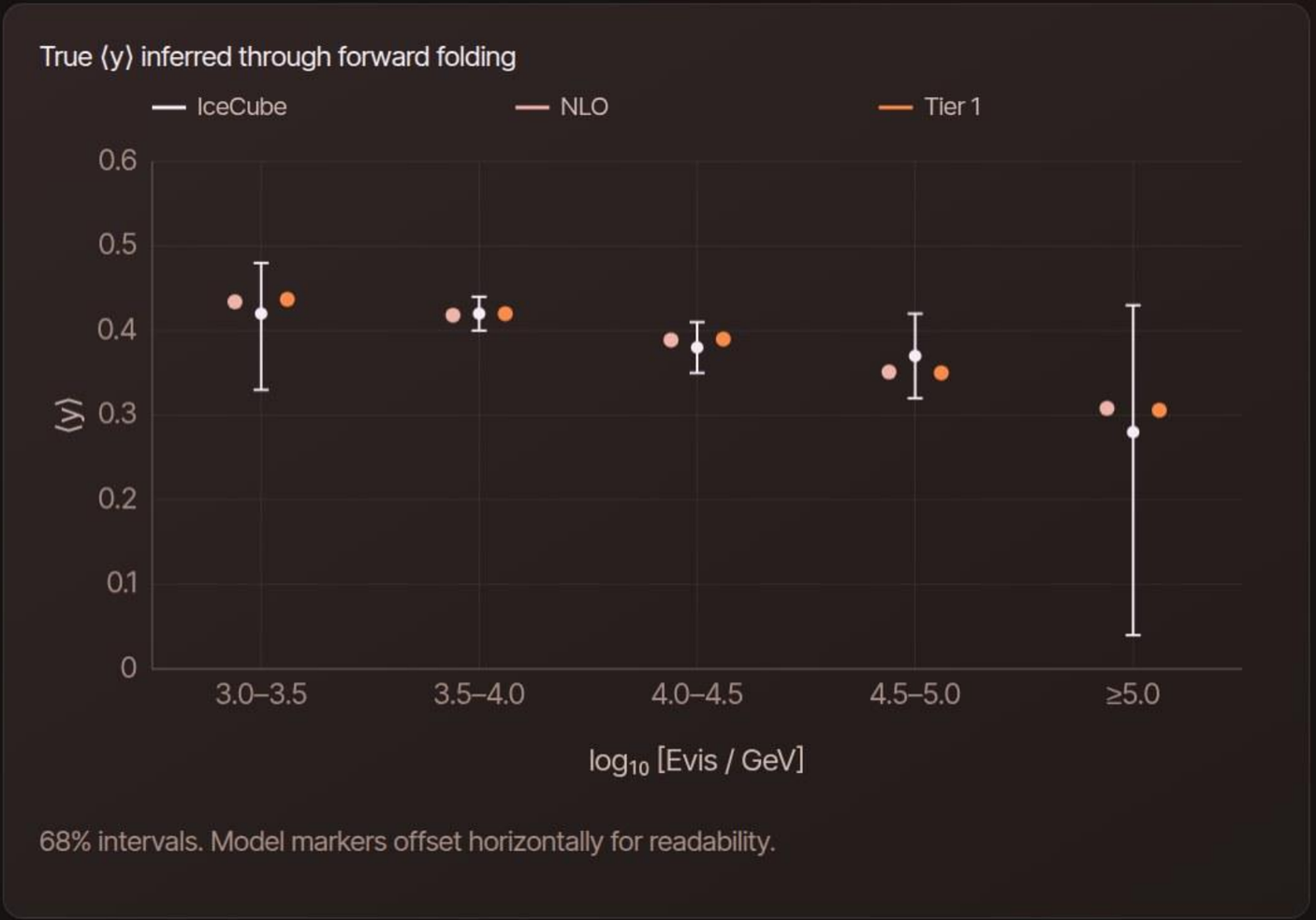
OBSERVATIONAL COMPARISON

The current measurement does not distinguish *the models*

All predictions lie within **0.6 times** the IceCube 68% half-interval.

Differences from the reference: ≤ 0.004 within the family and ≤ 0.011 for Bodek–Yang.

The chart shows the five visible-energy bins.



IceCube · arXiv:1808.07629 · Manuscript Table 6

COMPARISON VALIDATION

The forward fit preserves *the result*

TEST	RESULT
5 models, 11 responses, Asimov	FF − E1 = −0.003 … +0.004
Change in model differences	≤ 0.0006
300 pseudo-experiments per model, bins 1–4	Bias ≤ 0.001
Open bin, ~8 events	Bias up to 0.014; ~50% at boundaries

> The real IceCube response remains outside this test.

Manuscript §6 and appendix D.2 · VALIDATION §5f.1

DETECTOR LEVEL

The fit includes *flux and response*

$$N_{i,c}(b) = \int dE\, d\cos\theta\, dy\, \Phi_{i,c}\, P_i\, (d\sigma_i/dy)\, A_i\, M_i$$

Atmospheric and astrophysical fluxes, veto, Earth absorption, energy resolution and track selection.

> Acceptance was calibrated to IceCube counts after a first Asimov run had already shown the biases.

Calibration changes the shifts by less than 0.01 in r.

Manuscript · §7 · simplified response

FLUX RATIO

Shifts of *8% and up to 18%*

TRUTH ← TEMPLATES	ΔR	SHAPE PART
NLO ← Tier 1	−0.056	−0.025
Tier 1 ← NLO	+0.065	+0.030
NLO ← Tier 2 conv.	−0.107	−0.081
Tier 2 conv. ← NLO	+0.139	+0.103
NLO ← Bodek–Yang	+0.033	+0.091

> Asimov, r = 0.77. Tier 1–NLO: roughly half from shapes and half from cross sections and absorption.

Manuscript · Table 7 · complete configurations

STATISTICAL SCALE

Exposure makes *the difference relevant*

$$r = 0.77^{+0.32}_{-0.21}$$

Asimov profile at ×1, reference as truth

The error is asymmetric. The comparison uses the biased fit half-interval towards the true value.

×10 keeps the same response. It is not a specific Gen2 forecast.



Manuscript · §7, Comparison scale · interval ΔlnL = 1/2

FIT VALIDATION

Closure and coverage have *distinct scopes*

DIAGNOSTIC	×1	×10
Estimator $\hat{r}$	Upward bias of 6–10%	Diagnostics in $\rho = \ln r$
Closure in ρ	Fails; $\lvert\text{bias}\rvert \le 0.035$	0 failures in 65 tests
Profile coverage	Not evaluated	68.30 ± 0.23% / 95.01 ± 0.11%

> $\rho = \ln r$ was adopted after the failure. The transformation preserves the maximum and maps the interval.

Manuscript · §7.4 and appendix D.1

INTERPRETATION LIMITS

What the results *establish*

1

Differences between prescriptions

The family is finite and shares inputs. Its envelope has no probabilistic coverage.

2

Complete configurations in the detector

Nuclear and normalisation effects have not been separated at this level.

3

Inference in a proxy

The tests do not establish a bias in IceCube's measurement or validate its real response.

CONCLUSIONS

Composition inference requires *testing the distributions*

Similar means do not guarantee stable inferred composition.

0.12 → 0.008

decrease in ν–$\bar{\nu}$ separation

8–18%

r shifts within the family, in the proxy

0.8–1.6

times the profile error at ×10

SOURCES AND CREDITS

References and *data*

This work

R. C. R. de Lima and B. D. S. Moreira
Structure-function model dependence of the inelasticity of TeV–PeV neutrino interactions and of neutrino–antineutrino separation in neutrino telescopes
Manuscript in preparation, 30 October 2026 version.

Models

CSMS: JHEP 08 (2011) 042
BGK: Phys. Rev. D 66 (2002) 014001
GENIE and HEDIS: manuscript references.

IceCube

Phys. Rev. D 99 (2019) 032004
arXiv:1808.07629
icecube.wisc.edu/science/icecube

Images and numbers

IceCube Lab: John Hardin, CC BY 4.0.
Detector: K. Andeen and M. Plum, CC BY 4.0.
Study charts: SCARLET outputs, provenance in assets/data-sources.json.

SCARLET · TEV–PEV

Questions?

Inelasticity, composition and structure-function dependence

Rafael C. R. de Lima

rafael.lima@udesc.br

with Bruno Duarte da Silva Moreira · UDESC/CCT

rafael-lima.pages.dev/talks/scarlet